Official Journal of the World Water Council
Water Policy

Water Policy Vol 24 No 11, 1741 doi: 10.2166/wp.2022.065

Dynamic characteristics of drought conditions during the growth of summer maize

Bifeng Cui, Jianqin Ma*, Lei Liu, Xiuping Hao, Zhirui Song and Cheng Fang
North China University of Water Resources and Electric Power, Zhengzhou 450046, China
*Corresponding author. E-mail: majianqin@ncwu.edu.cn

ABSTRACT

This study aimed at investigating the applicability of a SWAT (Soil and Water Assessment Tool) model in understanding the effects of drought on summer maize. A real-time irrigation module was developed for the downstream irrigation area of the Yellow River to estimate the real-time irrigation of crops. By further simulating the dynamic evolution process of soil moisture content, a dynamic drought evaluation model of summer maize was established, and the relative soil moisture was set as the evaluation index to assess and analyze the dynamic variation of drought evolution during the growth of summer maize. The results showed that the improved SWAT model has strong applicability. During the growth of summer maize, the variation trend of drought is consistent with that of natural precipitation. Moreover, drought mainly occurs during the sowing-seedling and seedling-jointing stages, and the average frequency is 84.8 and 78.3%, respectively. Moderate drought is most likely to occur during the growth of summer maize and occurs mainly during the sowing-seedling and seedling-jointing stages, and the occurrence frequency is 55.3 and 32.6%, respectively. Extra-severe drought has the greatest impact, mainly in the jointing-tasseling, tasseling-milking and milking-maturity stages, and the occurrence frequency is 17.4, 15.2 and 10.9%, respectively.

Key words: downstream irrigation area of the Yellow River, dynamic characteristics of drought, improved SWAT model, real-time irrigation, relative soil moisture, summer maize

HIGHLIGHTS

- A real-time irrigation module was developed for the downstream irrigation area of the Yellow River to estimate the real-time irrigation of crops.
- We established a dynamic drought evaluation model of summer maize.
- We investigated the applicability of a SWAT model in understanding the effects of drought on summer maize.

GRAPHICAL ABSTRACT

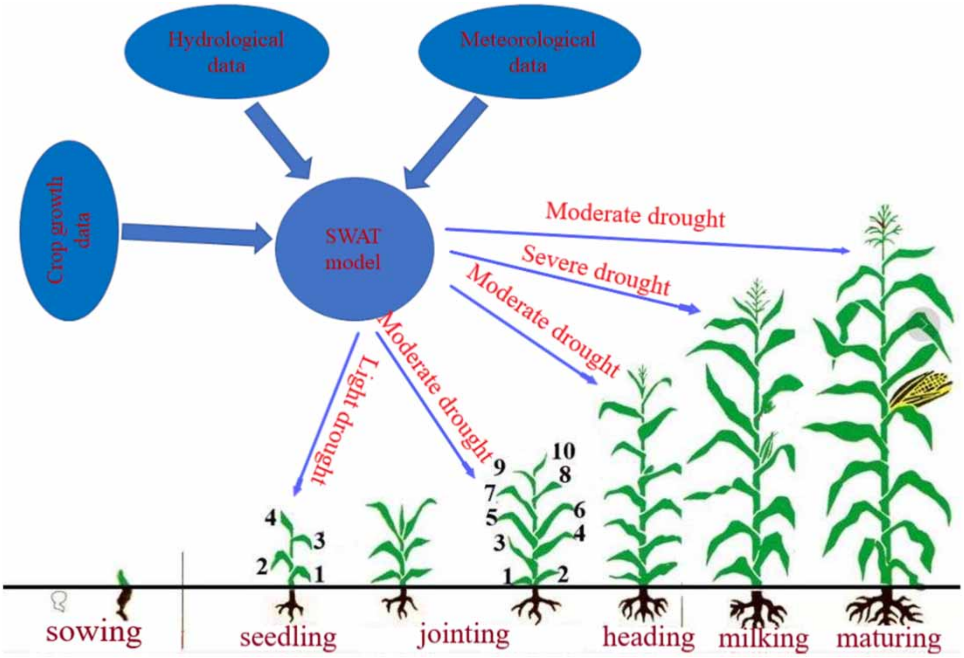

1. INTRODUCTION

Agricultural drought is defined as the phenomenon of reduction in the crop yield or even total crop failure due to the decrease in the soil moisture content during the crop growth period (Zhong *et al.*, 2016; Yonas, 2021), and it is one of the most serious natural disasters causing agricultural economic losses in China (Cui *et al.*, 2020). Previous studies indicate that the domestic agricultural aridity will be more severe in the following years in the context of climate change (Cho *et al.*, 2016; Zhang *et al.*, 2021). As the main crop in China, the growth process of summer maize is easily affected by agricultural drought events (Wu *et al.*, 2019). Consequently, the exploration of the drought process and its dynamic evolution during the crop growth period has great significance in preventing disastrous drought events and ensuring regional food security.

Agricultural dynamic drought refers to the process of describing the dynamic change of agricultural drought based on the real-time dynamic monitoring data of drought occurrence and development. Agricultural drought research based on real-time dynamic monitoring data can improve the accuracy of drought assessment (Kumar *et al.*, 2021; Prodhan *et al.*, 2021). The dynamic evaluation of agricultural drought is often completed through the evaluation of relative soil moisture, crop water deficit index and other indicators (Alam *et al.*, 2014). Presently, most of the real-time dynamic monitoring data for the research on agricultural drought are selected from various meteorological stations to build a crop drought evaluation index. By using a combination of methods such as long-term data analysis, mathematical model construction and comprehensive evaluation, the susceptibility of different crops to drought has been studied and analyzed on a temporal or spatial scale (Mishra & Singh, 2010; Xia *et al.*, 2018; Chen *et al.*, 2019; Li *et al.*, 2019; Zhang *et al.*, 2019). However, the meteorological stations in China are limited in number and uneven in geographic distribution. Therefore, the agricultural drought evaluation model that adopts meteorological data as source data often lacks space–time representativeness and shows unfavorable and unqualified accuracy in the regional agricultural drought research (Du *et al.*, 2014; Liu & Hwang, 2015; Wang *et al.*, 2018). However, the SWAT (Soil and Water Assessment Tool) distributed hydrological model can make up for this limitation (Xue *et al.*, 2019). By simulating the hydrological process of the watershed, the SWAT model can obtain continuous and large-scale hydrological and meteorological data of the studied area. Based on this rationale, researchers began to explore the application of the SWAT model in the crop water cycle process and irrigation water resources management from the early 21st century (Arnold *et al.*, 1998; Kumar & Kumar, 2020). As the research progressed, the SWAT model was employed in studies such as agricultural drought evaluation and understanding the dynamic changes of drought during the crop growth period, and was widely used in various climatic zones. The SWAT model can simulate the change of soil moisture content during crop growth period and calculate irrigation water (Wang *et al.*, 2003; Neitsch *et al.*, 2011; Cui *et al.*, 2018). For instance, McDaniel *et al.* (2017) adopted the SWAT model to simulate three drought indices, namely crop production, soil water consumption and transpiration during the growth season of cotton in the Upper Colorado River Basin (UCRB) and predicted the variation of agricultural drought for the next cropping season. By utilizing an improved SWAT model, Chen *et al.*, (2018) simulated the impact exerted by agricultural production practices on water saving and crop yield in the high plains of Texas. The results of their study indicated that a deep irrigation depth is favorable for maintaining the crop yield and reducing the occurrence of drought events. Sun *et al.* (2014) developed a drainage basin SWAT model and used it to simulate potential evapotranspiration and precipitation, which overcame the limitation of insufficient data from few meteorological stations located in complex terrain areas and enabled agricultural drought monitoring at the watershed scale. Li *et al.* (2014) and Wang *et al.* (2019) employed the SWAT model to simulate soil moisture content from which they calculated relative soil moisture and used it as an agricultural drought evaluation index. This allowed the evaluation of agricultural drought in areas where the soil moisture content data are absent.

However, in many of these previous studies, the effect by real-time irrigation on the precision of the SWAT model was not considered. Similarly, the dynamic changes in the extent of drought during the crop growth period under the combined effects of precipitation and irrigation were not included in the simulation. Additionally, there are very few studies on the dynamic characteristics of drought during the growth of summer maize in the downstream irrigation area of the Yellow River (Ma *et al.*, 2017, 2021). Therefore, a real-time irrigation module for the crop was developed in the SWAT model. Further, both the precipitation and the irrigation levels were adopted as the source of soil water during the growth of summer maize, which improved the soil water balance formula. The purpose is to allow simulation of the dynamic variation of the soil moisture during the growth of summer maize by constructing a drought evaluation model with relative soil moisture as the evaluation index. Furthermore, the dynamic variation of drought evolution during the whole growth period of summer maize was evaluated and analyzed to provide a theoretical background for the agricultural drought. The findings of this study can aid in the decision-making for the irrigation of downstream areas of the Yellow River.

2. MATERIALS AND METHODS

2.1. Study area

The Sanliuzhai Yellow River diversion irrigation area is located in Zhongmu County, Henan Province. The study area is situated downstream of the Yellow River which belongs to the warm temperate continental monsoon climate (Figure 1). The annual average temperature is 14.2 °C, and the annual average precipitation is 597.7 mm, which mainly occurs in summer, with seasonal drought. The annual farming period of the irrigation area is 309 days, the active growth period of crops is 217 days, and the frost-free period is 240 days. The irrigation area is an important grain and cotton production area, and suitable for the growth of various crops in Henan

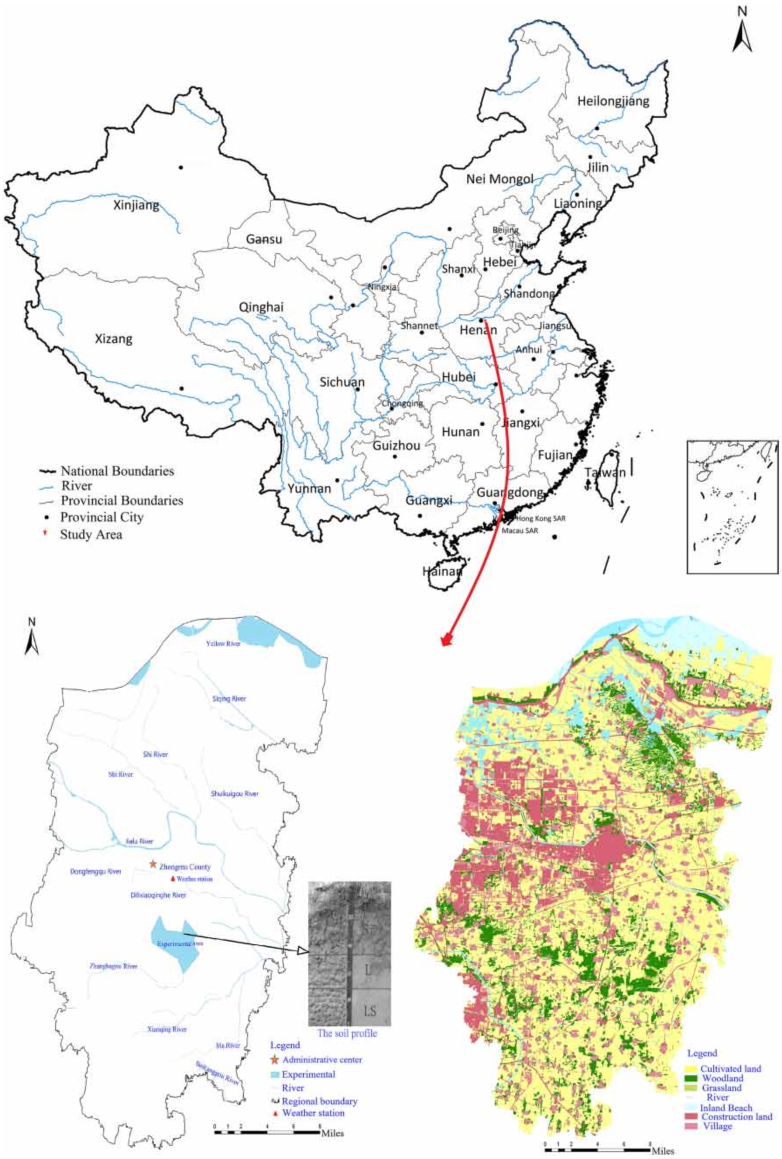

Fig. 1 | Location map of the study area.

Province. The irrigation water in the irrigation area is mainly from the Yellow River, with an irrigation area of 7,000 km^2, which belongs to a typical Yellow River Diversion Irrigation Area. Within 1 m, the soil types from top to bottom are silty soil, loamy soil and loam sandy soil (Bian *et al*., 2019; Henan Jiuzheng Engineering Consulting Co., Ltd, 2021).

In this study, the Sanliuzhai Yellow River irrigation area was taken as the research area, and the experiments were carried out in high-standard farmland, including soil moisture content and winter–summer maize index monitoring, etc.

2.2. Data source

The digital elevation model (DEM), land use status data and soil type data of the Sanliuzhai Yellow River diversion irrigation area were established based on the data coming from the Resources and Environment Data Center of the Chinese Academy of Sciences. The DEM data used were derived from 1:250,000 elevation data from the Re-source and Environment Data Center of the Chinese Academy of Sciences, and the resolution is 100 m. However, the soil hydraulic parameters were calculated and obtained from soil water characteristic software SPAW (Sachin *et al.*, 2014).

The data on variables such as precipitation, temperature, solar radiation, water consumption by vegetation, evaporation from land surfaces, wind direction and wind velocity were selected from the daily meteorological data of the Zhongmu national meteorological station from 1961 to 2017. The missing data were compensated by the built-in weather generator in the SWAT model. The crop growth parameters were determined and revised based on the built-in database in the SWAT model and also coordinating the actual growth pattern of the summer maize in the research area. The farmland management data were obtained from the literature review and field survey.

2.3. Improvement of the SWAT model

The SWAT model is a drainage basin distributed hydrological model featuring strong physical mechanism and is widely employed in agricultural water resources management, simulation of basin hydrological process and identifying agricultural non-point source pollution. The model is flexible and extensible, and it is computationally very efficient for doing continuous daily simulations for a longer period. However, the SWAT model cannot accurately simulate real-time crop water requirements (Harikrishna & Sanat, 2020; Navideh *et al.*, 2020; Ferreira *et al.*, 2021; Hanna *et al.*, 2021). Therefore, in this study, the following modifications were made to the SWAT model:

- The occurrence of drought events during the growth of summer maize is more susceptible to irrigation activities. In this study, a real-time crop irrigation module is developed in the SWAT model to simulate the real-time and dynamic impact exerted by irrigation activities on the irrigation district (Figure 2). Based on the real-time monitoring data of the soil moisture content, this module calculates the real-time soil moisture in the irrigation area and deduces the real-time water demand (M) of the crop according to current hydrological and meteorological data and crop growth conditions. Following that, the model compares the predicted precipitation (P) and the real-time water demand (M) and suggests if irrigation is required in the experimental region. If irrigation is required, the irrigation water shortage (WD) is calculated by subtracting real-time water demand (M) from predicted precipitation (P). If irrigation is not required, then the next HRU (Hydrologic Research Unit) will be activated. This module can accurately simulate the relative soil moisture and irrigate in real-time during the crop growth period, thus improving the accuracy of the simulation and making the results of this paper more accurate (Ma *et al.*, 2015).
- The soil water balance formula in the SWAT model was improved based on the real-time prediction of irrigated water shortage (WD), and the real-time irrigation amount was introduced as an index that can influence soil moisture content (Equation (1)). As the sources of water in the soil, both precipitation and irrigation levels were taken into consideration for studying the dynamic simulation of soil moisture content in the experimental area (Equation (2)).

The improved formula for water balance in the soil is as follows:

$$Irr = WD_1 + WD_2 + \ldots + WD_n \tag{1}$$

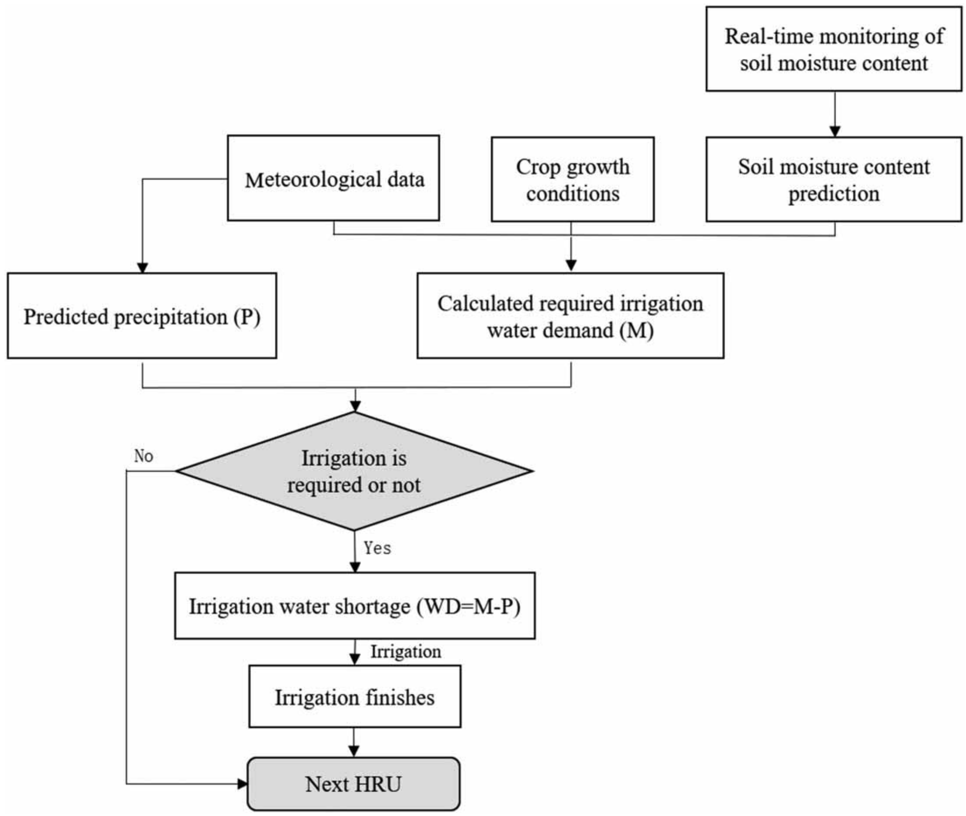

Fig. 2 | Structure of real-time irrigation module.

$$SW_t = SW_0 + \sum_{i=1}^{t} (Precip + Irr + Revap - ET_a - SURQ - PERC - LATQ - TILEQ) \quad (2)$$

where SW_t represents the final soil moisture content, and the unit is (mm). SW_0 represents the initial soil moisture content, and the unit is (mm). t represents the research period, and the unit is (s). *Precip* represents the effective precipitation levels during the research period, and the unit is (mm). *Irr* represents the irrigation levels during the research period, and the unit is (mm). *WD* represents the irrigation shortage quantity, and its unit is (mm). *Revap* is the potential transpiration capacity during the research period, and its unit is (mm). ET_a represents the actual transpiration capacity during the research period, and the unit is (mm). *SURQ* is the surface runoff amount during the research period, and the unit is (mm). *PERC* represents the infiltration quantity during the research period, and the unit is (mm). *LATQ* indicates the soil water flow during the research period, and its unit is (mm). *TILEQ* represents the drainage capacity of buried pipes during the research period, and the unit is (mm).

2.4. Rationality of calibration and validation of the SWAT model

2.4.1. Parameter calibration and verification of measured data

The SWAT-CUP was used for sensitivity analysis and verification based on the growth parameters and soil parameters of summer maize obtained from the field experiment in the middle and lower reaches of the Yellow River

(Luo *et al*., 2008; Liu & Luo, 2011). These parameters used in the SWAT model carried out calibration and verification with the help of the field test data of the study area such as actual measured output, soil moisture, leaf area index, etc. Following this, a verification experiment was carried out (Figure 3). The results indicated that the simulated soil moisture content was consistent with the measured value, and the actual dynamic change of soil moisture content could be reflected objectively by the simulated value of soil moisture content.

2.4.2. Validation of typical events

To ensure the feasibility of the improved SWAT model in drought research during the growth of the summer maize, typical drought events, as well as their development process in the experimental area, were adopted to verify the constructed model.

According to available information, a continuous drought during autumn and winter in 2008–2009 as well as in 2010–2011 and a summer drought in 2014 were observed and marked as severe drought events in recent years. By observing the experimental monitoring data during the above-mentioned drought events, it is clear that the precipitation in the experimental area was significantly low compared to previous years. From the experimental monitoring data, it is also apparent that the transpiration was greater than precipitation, and a large fluctuation in the soil moisture content was observed. The average values of relative soil moisture were 37.4, 21.9, and 33% during the above-mentioned drought events, and these events were graded as severe, extra-severe, and extra-severe, respectively. Even though extra irrigation water was supplied during these drought events, the drought state was often restored within 3–5 days of irrigation, particularly during the summer drought of 2014. This was because higher transpiration rates were usually observed in summer, and the variation of drought features was obvious despite intermittent precipitation (Ma, 2009; Duan *et al*., 2011; Li, 2014).

The SWAT model was utilized to assess and analyze the process of typical agricultural drought events, from the occurrence, development to termination (Figure 4). Compared with the actual experimental testing data, hydrometeorological data, and drought data, the simulation results were consistent with the actual development process of drought events.

Based on the research above, the accuracy of the method is verified by measured data and typical drought events. This means that the model can accomplish the drought event assessment in the experimental area, and

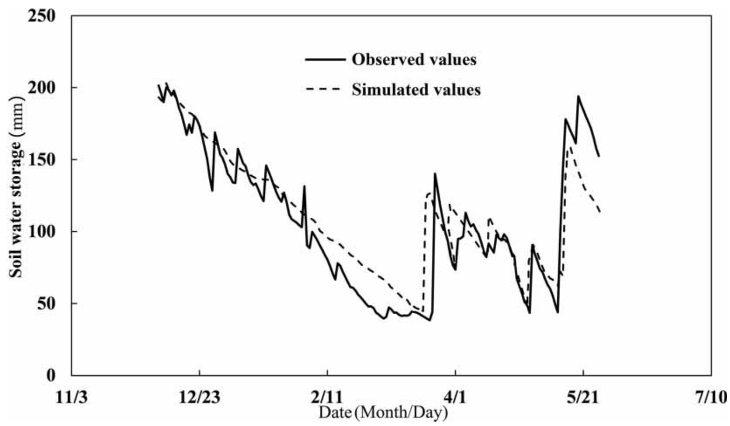

Fig. 3 | Comparison of measured and simulated soil moisture content during the field experimentation from December 10, 2015 to May 27, 2016.

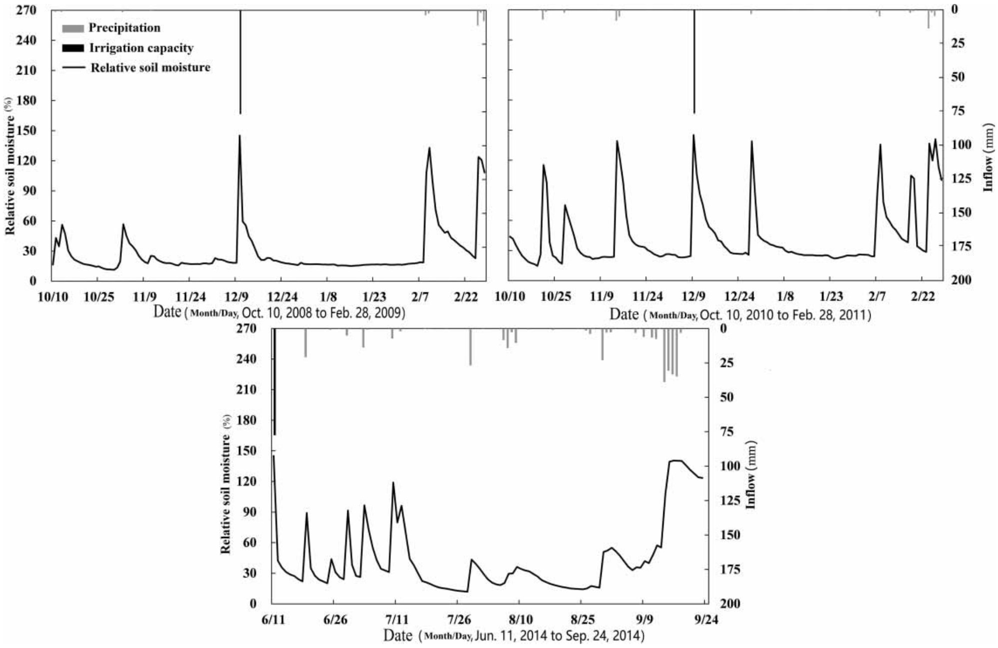

Fig. 4 | Variation of the daily relative soil moisture during typical drought events in the experimental area.

can also grade the drought event as well as provide the time scale for when the drought occurs, develops and finishes.

2.5. Assessment index and grading of agricultural drought

Usually, the soil moisture content simulated by the SWAT model is represented in mm. Therefore, it is required to convert the soil water storage into average soil weight moisture content (Sun *et al.*, 2014) (Equation (3)), which is used to calculate the relative soil moisture (Equation (4)).

$$\theta = \frac{SW}{d_{Z_{soil}} \times \rho_{soil} \times 10} \times 100\% \quad (3)$$

$$W = \frac{\theta}{F_c} \times 100\% \quad (4)$$

where W represents relative soil moisture, and the unit is (%). θ is the average soil weight moisture content (by weight), and its unit is (%). F_c is the field moisture capacity, and the unit is (%). SW is the moisture content of a certain deep soil layer simulated by hydrological model, and the unit is (mm). $d_{z_{soil}}$ is the thickness of the soil layer, and the unit is (cm). ρ_{soil} is soil bulk density, and the unit is (g/cm^3).

During the growth of summer maize, the root growth depth of summer maize is different at different growth stages, and the soil moisture content changes greatly at different depths. Based on the comprehensive analysis of the related results of drought indexes of summer maize, Xue *et al.* (2020) classified the soil depth and drought grade in different growth stages of summer maize (Table 1).

Table 1 | Drought index of maize based on relative soil moisture.

	Growth stages				
	Relative soil moisture (%)				
Drought grade	Sowing-seedling, 0–30 cm	Seedling-jointing, 0–30 cm	Jointing-tasseling, 0–60 cm	Tasseling-milking, 0–80 cm	Milking-maturity, 0–60 cm
Free drought	>65	>60	>70	>75	>70
Light drought	>55–65	>50–60	>60–70	>65–75	>60–70
Middle drought	>45–55	>40–50	>50–60	>55–65	>50–60
Severe drought	>40–45	>35–40	>45–50	>50–55	>45–50
Extra-severe drought	≤40	≤35	≤45	≤50	≤45

3. RESULTS AND DISCUSSIONS

3.1. Dynamic characteristics of drought events during the growth of summer maize

3.1.1. Variation characteristics of relative soil moisture during different growth stages of summer maize

The improved SWAT model was employed to simulate the relative soil moisture during the whole growth stage of summer maize from 1972 to 2017 and the results were used to compare with the corresponding precipitation (Figure 5).

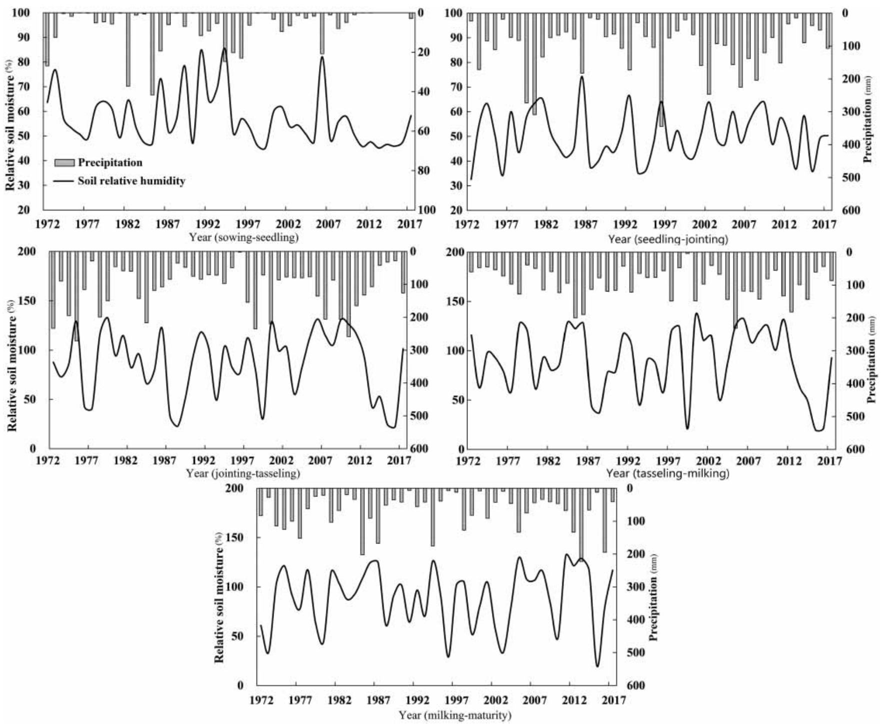

Fig. 5 | Change in annual precipitation and relative humidity during the whole growth period of summer maize from 1972 to 2017.

During the sowing-seedling stage, the average relative soil moisture was 57.0%, with a maximum value of 85.2% and a minimum value of 45.1%. The corresponding precipitation during this stage was 24.7 and 0 mm and the precipitation frequency was 22.6 and 99.7%, respectively, and the interannual variation coefficient of precipitation was 0.19. While the average annual precipitation during the same stage was 7.3 mm which varied from 0 to 41.6 mm, with the interannual variation coefficient of 1.39.

During the seedling-jointing stage, the average relative soil moisture was 50.4%, with a maximum value of 75.3% and a minimum value of 32.6%. The precipitation corresponding during this stage was 182.3 and 23.9 mm, the precipitation frequency was 14.9 and 87.2%, respectively, and the interannual variation coefficient of precipitation was 0.20. While the average annual precipitation during the same stage was 107.6 mm which varied from 13.9 to 344.5 mm, with an interannual variation coefficient of 0.73.

During the jointing-tasseling stage, the average relative soil moisture was 86.2%, with a maximum value of 132.7% and a minimum value of 22.8%. The precipitation corresponding during this stage was 149.7 and 34.9 mm and the precipitation frequency was 27.7 and 89.4%, respectively, and the interannual variation coefficient was 0.38. While the average annual precipitation during the same stage was 115.2 mm which varied from 1.6 to 271.5 mm, with an interannual variation coefficient of 0.61.

During the tasseling-milking stage, the average relative soil moisture was 90.1%, with a maximum value of 135.2% and a minimum value of 19.8%. The precipitation corresponding during this stage was 148.3 and 60.5 mm, the precipitation frequency was 12.8 and 68.1%, respectively, and the interannual variation coefficient was 0.37. While the average annual precipitation in the same stage was 96.3 mm which varied from 3.7 to 231.3 mm, with an interannual variation coefficient of 0.51.

During the milking-maturity stage, the average relative soil moisture was 89.7%, with a maximum value of 131.6% and a minimum value of 19.7%. The precipitation corresponding during this stage was 67.6 and 11.9 mm and the precipitation frequency was 40.4 and 87.2%, respectively, and the interannual variation coefficient was 0.34. While the average annual precipitation in the same stage was 77.4 mm which varied from 3.0 to 105.3 mm, with an interannual variation coefficient of 0.78.

Consequently, during the growth of summer maize from 1972 to 2017, the average relative soil moisture was largely influenced by precipitation. The variation trend of relative soil moisture corresponded well with the dynamic variation trend of precipitation. Subsequently, Pearson's correlation analysis was carried out for each growth stage. Results indicated that the correlation coefficient was between 0.41 and 0.71, and both passed the significance test in which $\alpha = 0.01$ (Su *et al.*, 2020). This suggests that rainfall was the main source that replenishes soil moisture during the growth of summer maize in the experimental area. However, relatively high correlation coefficients were observed during the jointing-tasseling stage, which is 0.71, and were relatively lower at other growth stages, which is about 0.5. This is because the soil depth of relative soil moisture considered by summer maize at different growth stages is different, and the correlation coefficient between relative soil moisture and precipitation is inversely proportional to the depth of the soil layer considered. The deeper the depth of the soil layer considered, the smaller the correlation coefficient between the two, and the smaller the influence of precipitation on relative soil moisture. Although the soil depth in the sowing-seedling stage is 0–30 cm, its correlation coefficient is only 0.45, mainly because the sowing-seedling stage is relatively short, the relative soil moisture is greatly affected by the early precipitation, and the correlation coefficient with the corresponding precipitation is relatively small.

3.1.2. Interannual variation and frequency of drought during different growth stages of summer maize

The interannual variation, linear variation, and 5-year moving average trend of relative soil moisture at each growth stage of summer maize in the experimental area from 1972 to 2016 are shown in Figure 6. The relative soil moisture at different growth stages of summer maize followed in cyclic fluctuation of 'ascend–descend–ascend'.

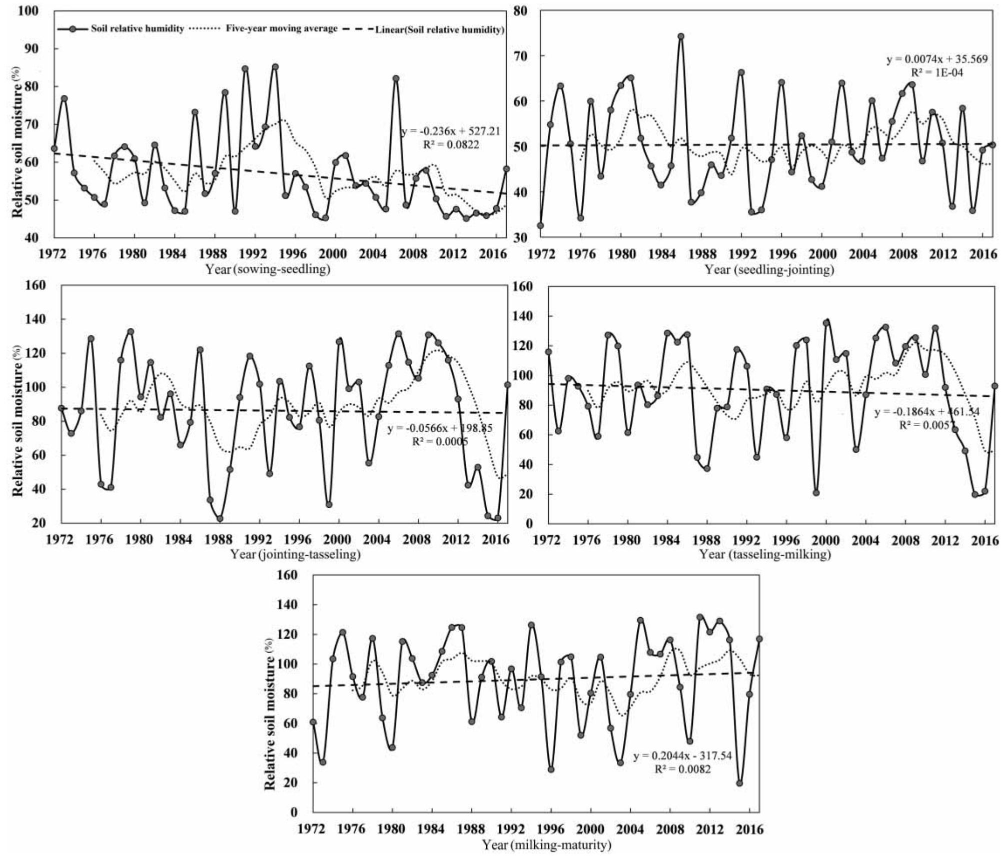

Fig. 6 | Variation tendency of annual relative humidity during the whole growth period of summer maize from 1970 to 2016.

By analyzing the total variation trend of relative soil moisture during each growth stage, it was noted that the change range of relative soil moisture is small in the sowing-seedling and seedling-jointing stages, but relatively large in the jointing-tasseling, tasseling-milking, and milking-maturity stages, and the years of drought in each growth stage were different.

By conducting the linear trend analysis of relative soil moisture, there was no significant change in relative soil moisture at the seedling-jointing and jointing-tasseling stages, that is, the drought conditions for many years remained basically unchanged in these two growth stages. However, it was observed that the overall relative soil moisture decreased at the rate of 2.36 every 10 years and 1.86 every 10 years during the sowing-tillering and tasseling-milking stages, respectively. This indicated that the degree of drought in the experimental area showed an aggravating trend during these two growth stages. In addition, the overall relative soil moisture increased at the rate of 2.04 every 10 years during the milking-maturity stage. This implied that the degree of drought in the experimental area showed an ameliorating trend during this growth stage. Employing the M–K trend analysis of relative soil moisture at each growth stage, only the sowing-tillering passed the significance test where $\alpha = 0.05$ (Adam *et al.*, 2020). This indicates that in the long term, the variation of relative soil moisture during the growth of summer maize became more stable, or in other words, the variation of extent of drought degree remained steady during the growth stage of summer maize in the experimental area.

Correlation analysis showed a positive correlation between 5-year moving average curve and the variation trend of relative soil moisture during each growth stage of summer maize. Moreover, the variation trend of relative soil moisture changed significantly during the jointing-tasseling and tasseling-milking stages, while a relatively small fluctuation was observed during the sowing-seedling, seedling-jointing, and milking-maturity stages. This indicated that during the experimental stage, the drought severity on summer maize was relatively significant during the jointing-tasseling and tasseling-milking stages.

To further understand the drought characteristics of summer maize, the frequency of drought during different growth stages of summer maize from 1972 to 2017 was calculated. The average frequency of drought in each growth stage of summer maize was 84.8, 78.3, 28.3, 28.3 and 26.1%, respectively. By analyzing the frequency of drought in each growth stage of summer maize, light drought and moderate drought occurred mainly in the sowing-seedling stage, with frequencies of 30.4 and 55.3%, respectively. At the same time, light drought, moderate drought and severe drought were the main types in the seedling-jointing stage, and the occurrence frequencies were 28.3, 32.6 and 13.0%, respectively. Also, during the jointing-tasseling stage, extra-severe drought mainly occurred, and the frequency was 17.4%. Similarly, only moderate drought, severe drought and extra-severe drought occurred during the tasseling-milking stage, and the occurrence frequencies were 10.9, 2.2 and 15.2%, respectively. In the end, the frequency of light drought was 8.7% and that of extra-severe drought was 10.9% during the milking-maturity stage.

These observations indicate that summer maize is susceptible to drought during the sowing-seedling stage and the seedling-joining stage, and the frequency of light drought and moderate drought are relatively high. Nevertheless, extra-severe drought is most likely to occur during the jointing-tasseling, tasseling-milking, and milking-maturity stages. This is because the frequency of precipitation increases in the middle and late growth period of summer maize, which reduces the possibility of drought. In addition, due to the high temperature in summer, if there is no effective rainfall, the strong evaporation and transpiration can easily cause serious drought problems.

3.2. Spatial distribution characteristics of drought in summer maize

Spatially, the drought status of summer maize in the study area has little change, and the annual average drought frequency is between 25.6 and 37.7%. As the study area is north–south, the study is divided into three regions on average: north, central and south. The drought frequency of summer maize is 33.8–37.7%, 28.9–34.2% and 25.6–30.1%, respectively (Figure 7). The agricultural drought trend weakens from north to south because the rivers in the study area mainly flow through the southern region, and the largest river Jialu river flows through the middle and south.

3.3. Planting experiment of summer corn

The SWAT model studied in this paper was used to conduct summer maize planting tests from 2015 to 2016. The test was divided into a real-time irrigation group and a conventional irrigation group. The real-time irrigation group was irrigated according to the dynamic drought law of summer maize growth period and real-time soil water content, and the conventional irrigation group was irrigated according to planting experience. The test results show that the water consumption of each growth stage of the real-time irrigation group is smaller than that of the conventional irrigation group. The total water consumption decreased by 450.23 and 500.25 m^3/ha in 2015 and 2016, while the yield increased by 361.95 and 347.1 kg/ha, and water use efficiency (WUE) increased by 0.24 and 0.25, respectively (Table 2). This is because the real-time irrigation group can conduct timely and appropriate irrigation for summer maize, which reduces the drought risk of summer maize and avoids the yield reduction of summer maize caused by excessive irrigation. Therefore, the SWAT model studied in this paper can reduce the consumption of soil moisture and improve the yield of summer maize.

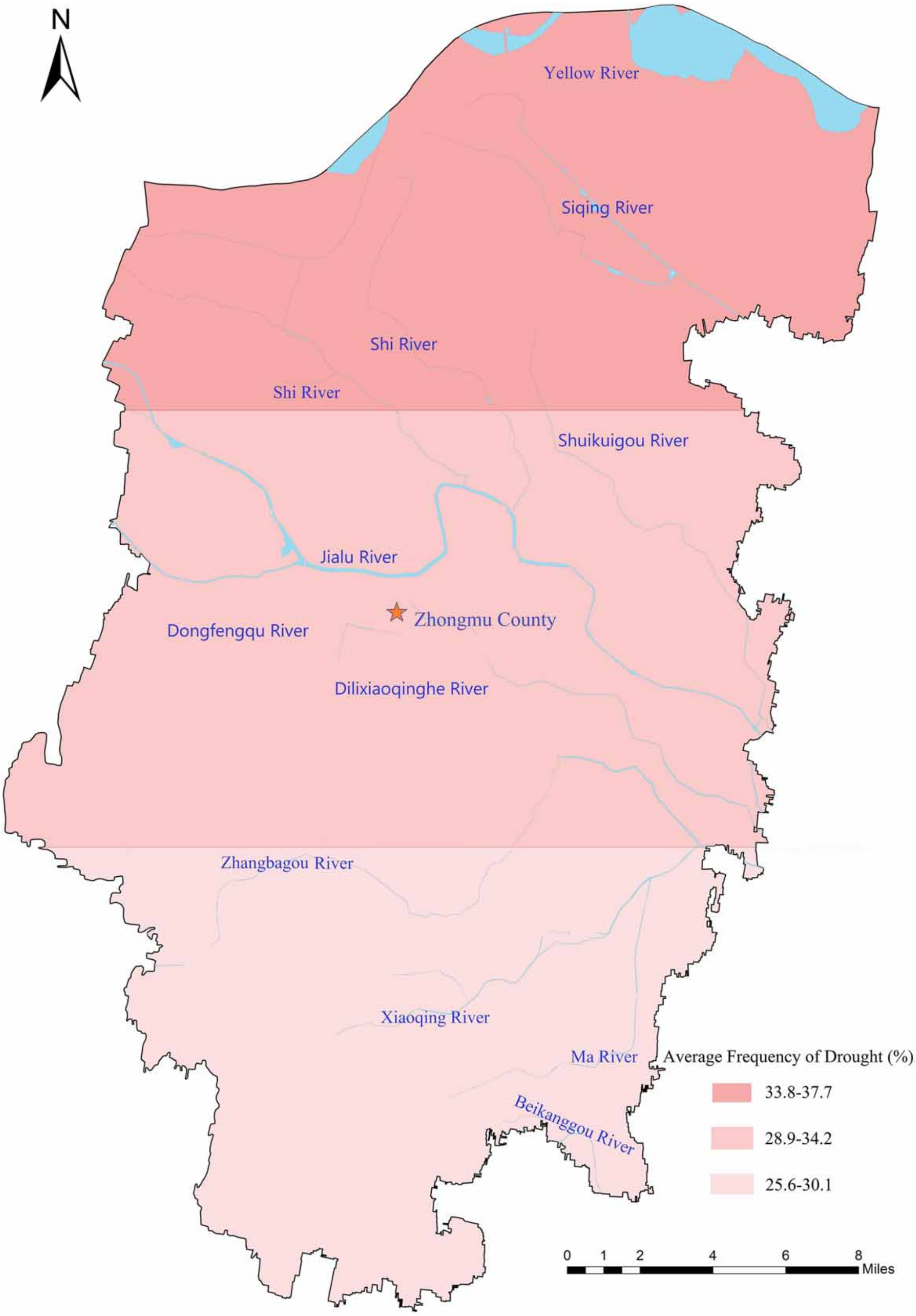

Fig. 7 | Annual drought frequency distribution of summer maize.

Table 2 | Test results of summer maize planting.

Year	Test scheme	Water consumption (m^3/ha)						Irrigation amount (m^3/ha)	Yield (kg/ha)	WUE
		Sowing-seedling	Seedling-jointing	Jointing-tasseling	Tasseling-milking	Milking-maturity	Growth period			
2015	Real-time irrigation group	337.67	839.72	1,272.24	952.88	1,283.94	4,686.44	1,400.70	8,862.00	1.89
	Conventional irrigation group	387.69	939.77	1,372.29	1,052.93	1,383.99	5,136.67	1,850.93	8,500.05	1.65
2016	Real-time irrigation group	306.95	933.07	1,174.79	1,058.73	1,396.20	4,869.73	1,300.65	9,847.05	2.02
	Conventional irrigation group	356.98	1,043.12	1,284.84	1,168.78	1,516.26	5,369.98	1,800.90	9,499.95	1.79

4. CONCLUSIONS

A real-time irrigation module was developed in the SWAT model, and thus the soil water balance formula was improved. By simulating the soil moisture content in the experimental area, the relative soil moisture during the growth period of summer maize was calculated. Then, the results were adopted as the assessment indices and were utilized to evaluate and analyze the dynamic characteristics of drought during different growth stages of summer maize. The following conclusions were made from this study.

The drought conditions during the growth of summer maize were greatly affected by precipitation, and the variation trend of drought remains stable in long term and the interannual variation is significant. During each growth period, the dynamic variation trend of average relative soil moisture kept consistent with corresponding precipitation. Their correlation coefficients ranged between 0.612 and 0.761, and they all passed the significance test where $\alpha = 0.01$. In addition, the soil relative humidity of summer maize at the seedling-joining and jointing-tasseling stages varies greatly in different years, with the change of rainfall.

During each growth stage of summer maize, drought could be easily observed, and mainly in moderate drought and light drought with the annual average drought frequency was between 10.9–55.3% and 8.7–30.4%, respectively. Nevertheless, severe drought and extra-severe drought are mostly observed during the jointing-tasseling, tasseling-milking, and milking-maturity stages, and the annual average drought frequency was between 2.2–13.0% and 10.9–17.4%, respectively. Spatially, the annual average drought frequency of summer maize is between 25.6 and 37.7%, and the drought gradually weakened from north to south.

The improved SWAT model has demonstrated strong applicability in the study of drought conditions during the growth of summer maize. This improved model can provide a novel approach for researching the dynamic characteristics of summer maize drought conditions. This study can also offer a scientific basis for preventing agricultural drought downstream of the Yellow River where the irrigation district resides.

DATA AVAILABILITY STATEMENT

All relevant data are included in the paper or its Supplementary Information.

CONFLICT OF INTEREST

The authors declare there is no conflict.

REFERENCES

Adam, P., Leszek, S. & Dariusz, W. (2020). Spatial differentiation of the maximum river runoff synchronicity in the Warta River Catchment, Poland. *Water 12*(6), 1782.

Alam, A., Saadat, A., Rahman, M. & Rahman, S. (2014). Spatio-temporal variation of agricultural drought in the Barind region of Bangladesh: an application of a Markov Chain model. *Irrigation and Researcher 63*(3), 383–393.

Arnold, J., Srinivasan, R., Muttiah, R. & Williams, J. (1998). Large area hydrologic modeling and assessment part I: model development. *Jawra Journal of the American Water Resources Association 34*(1), 73–89.

Bian, Y., Huang, F. & Cao, H. (2019). Analysis of diversion capacity of Sanliuzhai irrigation area on the lower Yellow River. *Yellow River 41*(01), 152–156.

Chen, Y., Marek, G. & Marek, T. (2018). Improving SWAT auto-irrigation functions for simulating agricultural irrigation management using long-term lysimeter field data. *Environmental Modelling and Software 99*, 25–38.

Chen, S., Thian, Y. & Tan, X. (2019). Assessment of CFSR, ERA-Interim, JRA-55, MERRA-2, NCEP-2 reanalysis data for drought analysis over China. *Climate Dynamics 53*(1), 737–757.

Cho, J., Ko, G., Kim, K. & Oh, C. (2016). Climate change impacts on agricultural drought with consideration of uncertainty in CMIP5 scenarios. *Irrigation and Drainage 65*(2), 7–15.

Cui, Y., Wu, D. & Wang, S. (2018). Simulation and analysis of irrigation water consumption in multi-source water irrigation districts in Southern China based on modified SWAT model. *Transactions of the Chinese Society of Agricultural Engineering 34*(14), 94–100.

Cui, Y., Zhang, B., Huang, H., Wang, X., Zeng, J., Jiao, W. & Yao, R. (2020). Identification of seasonal sub-regions of the drought in the North China Plain. *Water 12*(12), 3447–3447.

Du, L., Tian, Q. & Wang, L. (2014). A synthesized drought monitoring model based on multi-source remote sensing data. *Transactions of the Chinese Society of Agricultural Engineering 30*(09), 126–132.

Duan, H., Wang, S. & Feng, J. (2011). National drought situation in 2010 and its influence and causes. *Journal of Arid Meteorology 29*(01), 126–132.

Ferreira, A., Almeida, A., Koide, S., Minoti, R. & Siqueira, M. (2021). Evaluation of evapotranspiration in Brazilian Cerrado Biome simulated with the SWAT model. *Water 13*(15), 2037–2037.

Hanna, K., Paul, M., NegahbanAzar, M. & Shirmohammadi, A. (2021). Developing a decision support system for economic analysis of irrigation applications in temperate zones. *Water 13*(15), 2044–2044.

Harikrishna, S. & Sanat, N. (2020). A methodological framework for identification of baseline scenario and assessing the impact of DEM scenarios on SWAT model outputs. *Water Resources Management 34*(15), 4795–4814.

Henan Jiuzheng Engineering Consulting Co., Ltd. (2021). *Preliminary Design Text of 666.7 Hectares High Standard Farmland Con-Struction Project in Yaojia Town, Zhongmou County in 2021*. Henan Jiuzheng Engineering Consulting Co., Ltd, Zhengzhou, pp. 17–25.

Kumar, D. & Kumar, B. (2020). Evaluating two GIS-based semi-distributed hydrological models in the Bhagirathi-Alkhnanda River catchment in India. *Water Policy 22*(6), 991–1014.

Kumar, U., Singh, S., Bisht, J. & Kant, L. (2021). Use of meteorological data for identification of agricultural drought in Kumaon region of Uttarakhand. *Journal of Earth System Science 130*(3), 1–13.

Li, Z. (2014) Nearly 35% of small reservoirs in Henan suffered the worst drought in 63 years [EB/OL]. 2014-07-28. Available from: http://news.youth.cn/gn/201407/t20140728_5568520.htm.

Li, Y., Liang, Z. & Zhao, W. (2014). Evaluation method and its application of agricultural drought based on SWAT model. *South-to-North Water Transfers and Water Science & Technology 12*(01), 7–11.

Li, F., Li, H. & Lu, W. (2019). Meteorological drought monitoring in northeastern China using multiple indices. *Water 11*(1), 72–92.

Liu, Y. & Hwang, Y. (2015). Improving drought predictability in Arkansas using the ensemble PDSI forecast technique. *Stochastic Environmental Research and Risk Assessment 29*(1), 79–91.

Liu, L. & Luo, Y. (2011). Effects of different irrigation systems on the relationship between crops and water in the irrigation districts along the lower reaches of the Yellow River. *Journal of Irrigation and Drainage 30*(01), 5–10.

Luo, Y., He, C. & Sophocleous, M. (2008). Assessment of crop growth and soil water modules in SWAT2000 using extensive field experiment data in an irrigation district of the Yellow River Basin. *Journal of Hydrology 352*(1-2), 139–156.

Ma, J. (2009) Zhengzhou suffered the worst drought in 50 years, 1.67 million mu of farmland and 130000 people were affected [EB/OL]. 2009-02-05. Available from: http://finance.ifeng.com/a/20090205/352190_0.shtml.

Ma, J., He, S. & Song, Z. (2015). Calculation method of soil moisture content in crop root and its application in the real-time irrigation model. *Journal of Irrigation and Drainage 34*(04), 19–23.

Ma, J., Cui, B. & Liu, L. (2017). Application of fuzzy comprehensive evaluation based on improved analytic hierarchy process in optimization of irrigation scheme. *Water Saving Irrigation 8*, 34–37 + 43.

Ma, J., He, Q. & Liu, L. (2021). Optimizing irrigation and fertilization coupling to balance the improvement of yield and water use efficiency of summer maize. *Journal of Irrigation and Drainage 40*(10), 58–63.

McDaniel, R., Munster, C. & Nielsen-Gammon, J. (2017). Crop and location specific agricultural drought quantification: PART III. *Forecasting water stress and yield trends. Biotech Week 60*(03), 741–752.

Mishra, A. & Singh, V. (2010). A review of drought concepts. *Journal of Hydrology 391*(1), 202–216.

Navideh, N., Latif, K. & Sabahattin, I. (2020). Water quality prediction using SWAT-ANN coupled approach. *Journal of Hydrology 590*, 125220.

Neitsch, S., Arnold, J. & Kiniry, J. (2011). *Soil and Water Assessment Tool Theoretical Documentation, Version 2009*. Texas Water Resources Institute, Texas.

Prodhan, F., Zhang, J. & Yao, F. (2021). Deep learning for monitoring agricultural drought in south Asia using remote sensing data. *Remote Sensing 13*(9), 1715–1715.

Sachin, N., Ashwini, K. & Sangita, S. (2014). Soil erodibility estimation for soil conservation in dapoli region of Maharashtra. *Trends in Biosciences 7*(6), 486–490.

Su, Y., Li, W., Liu, L., Li, J., Sun, X. & Hu, W. (2020). Assessment of medium and small river health based on macroinvertebrates habitat suitability curves: a case study in a tributary of Yangtze River, China. *Water Policy 22*(4), 602–621.

Sun, L., Chen, X. & Pei, Z. (2014). Drought monitoring of upper and middle reaches of Qingjiang Basin based on SWAT model. *Transactions of the Chinese Society of Agricultural Engineering 30*(21), 129–137.

Wang, Z., Liu, C. & Huang, Y. (2003). The theory of SWAT model and its application in Haihe Basin. *Progress in Geography 22*(1), 79–86.

Wang, W., Huang, J. & Cui, W. (2018). Comparison of drought indices for remote sensing drought monitoring in Yunnan-Guizhou Plateau region. *Transactions of the Chinese Society of Agricultural Engineering 34*(19), 131–139 + 309.

Wang, F., Wang, J. & Shi, J. (2019). Study on simulation of agricultural drought in a region based on SWAT model. *Journal of North China University of Water Resources and Electric Power (Natural Science Edition) 40*(01), 64–70.

Wu, X., Wang, P., Gong, Y. & Yang, J. (2019). Analysis of drought identification and spatio-temporal characteristics for summer corn in huang-Huai-Hai plain in year of 1961 - 2015. *Transactions of the Chinese Society of Agricultural Engineering 35*(18), 189–199.

Xia, L., Zhao, F. & Mao, K. (2018). SPI-Based analyses of drought changes over the past 60 Years in China's major crop-growing areas. *Remote Sensing 10*, 171–186.

Xue, F., Shi, P., Qu, S., Wang, J. & Zhou, Y. (2019). Evaluating the impact of spatial variability of precipitation on streamflow simulation using a SWAT model. *Water Policy 21*(1), 178–196.

Xue, C., Zhang, Y. & Liu, W. (2020). Spatial and temporal characteristics of extreme drought in summer maize growing season in Henan Province during 1971–2016. *Agricultural Research in the Arid Areas 38*(02), 258–266 + 275.

Yonas, T. (2021). Perception of agricultural drought resilience in South Africa: a case of smallholder livestock farmers. *Jàmbá: Journal of Disaster Risk Studies 13*(1), e1–e11.

Zhang, R., Chen, Z. & Xu, L. (2019). Meteorological drought forecasting based on a statistical model with machine learning techniques in Shaanxi province, China. *Science of the Total Environment 665*, 338–346.

Zhang, Y., Hao, Z., Feng, S., Zhang, X., Xu, Y. & Hao, F. (2021). Agricultural drought prediction in China based on drought propagation and large-scale drivers. *Agricultural Water Management 255*, 107028.

Zhong, S., Sha, J. & Shen, L. (2016). Measuring drought based on a CGE model with multi-regional irrigation water. *Water Policy 18*(4), 877–891.

First received 26 March 2022; accepted in revised form 25 September 2022. Available online 11 October 2022